European Journal of Medicinal Chemistry 203 (2020) 112574

Contents lists available at ScienceDirect

European Journal of Medicinal Chemistry

journal homepage: http://www.elsevier.com/locate/ejmech

Research paper

Optimization of IEDDA bioorthogonal system: Efficient process to improve trans-cyclooctene/tetrazine interaction

Jean-Baptiste Béquignat [a, b, c, 2], Nancy Ty [a, b, c, 2], Aurélie Rondon [a, b, c, d, 1], Ludivine Taiariol [a, b, c], Françoise Degoul [a, b, c], Damien Canitrot [a, b, c], Mercedes Quintana [a, b, c], Isabelle Navarro-Teulon [d], Elisabeth Miot-Noirault [a, b, c], Claude Boucheix [e], Jean-Michel Chezal [a, b, c], Emmanuel Moreau [a, b, c, *]

[a] Université Clermont Auvergne, Imagerie Moléculaire et Stratégies Théranostiques, BP 184, F-63005, Clermont-Ferrand, France
[b] Inserm, U 1240, F-63000, Clermont-Ferrand, France
[c] Centre Jean Perrin, F-63011, Clermont-Ferrand, France
[d] Institut de Recherche en Cancérologie (IRCM), U1194 — Université Montpellier — ICM, Radiobiology and Targeted Radiotherapy, 34298, Montpellier Cedex 5, France
[e] INSERM, UMR-S 935, Villejuif, France

ARTICLE INFO

Article history:
Received 21 February 2020
Received in revised form
11 June 2020
Accepted 11 June 2020
Available online xxx

Keywords:
Bioorganic chemistry
Pretargeting
Trans-cyclooctene
TCO isomerization
PEGylated linkers synthesis

ABSTRACT

The antibody pretargeting approach for radioimmunotherapy (RIT) using inverse electron demand Diels-Alder cycloaddition (IEDDA) constitutes an emerging theranostic approach for solid cancers. However, IEDDA pretargeting has not reached clinical trial. The major limitation of the IEDDA strategy depends largely on trans-cyclooctene (TCO) stability. Indeed, TCO may isomerize into the more stable but unreactive cis-cyclooctene (CCO), leading to a drastic decrease of IEDDA efficiency. We have thus developed both efficient and reproducible synthetic pathways and analytical follow up for (PEGylated) TCO derivatives, providing high TCO isomeric purity for antibody modification. We have set up an original process to limit the isomerization of TCO to CCO before the mAbs' functionalization to allow high TCO/tetrazine cycloaddition.

1. Introduction

Radioimmunotherapy (RIT) consists in treating tumors using monoclonal antibodies (mAbs) radiolabeled with β- or α-emitting radionuclide, either directly (e.g. radioiodination on tyrosine residues) or through a radiolabeled prosthetic group (most notably couplings between N-hydroxysuccinimidyl (NHS) esters and lysines or hetero-Michael additions between maleimides and thiol group of cysteine residues). RIT efficiency has been well established in hematological diseases, such as Non-Hodgkin Lymphoma with the approval in 2002 of ibritumomab tiuxetan (Zevalin®, Bayer). However, RIT of solid tumors faces two major drawbacks, namely poor mAb diffusion in tumors and hematotoxicity caused by their slow blood clearance [1,2]. Recent advances have led to the development of pretargeting approaches (PRIT) to limit irradiation of healthy tissues (Fig. 1A) [3,4].

Unlike RIT, PRIT relies on a specific recognition between a functionalized mAb and a fast blood cleared radiolabeled probe, injected 24–48 h after the modified mAb. However, only few PRIT approaches have so far been investigated in clinical trials [5–7]. The (strept)avidin-biotin system, which was the first PRIT system assessed in humans, demonstrated important (strept)avidin-based immunogenicity and non-specific interaction with endogenous biotin. The bispecific antibodies/hapten system successfully reached phase II/III but requires a long and expensive engineering [8–14]. Copper-free click chemistry strategies offer an attractive alternative due to their selectivity, fast reaction rate, ease and modularity of ligation, particularly for the "second generation" bioorthogonal reactions. These stand out by their fast reaction

* Corresponding author. UMR 1240, IMOST, Univ. Clermont Auvergne, INSERM, 58 rue Montalembert, F-63005, Clermont-Ferrand, France.
E-mail address: emmanuel.moreau@uca.fr (E. Moreau).
[1] Present address: Université Catholique de Louvain, Louvain Drug Research Institute, ADDB, 73 avenue Mounier, 1200 Bruxelles, Belgique.
[2] These authors contributed equally.

https://doi.org/10.1016/j.ejmech.2020.112574
0223-5234/

kinetics under physiological conditions (solvent, pH and temperature). Bioorthogonal chemistry is also characterized by the absence of side reactions between bioorthogonal entities and biological macromolecules, thus ensuring biocompatibility in living systems. This led to the development of a dozen of reactions where the most promising appeared to be strained-promoted alkyne-azide cycloaddition (SPAAC) and the inverse electron-demand Diels-Alder (IEDDA) cycloaddition based on trans-cyclooctene (TCO)/tetrazine (Tz) conjugation [15–18]. For PRIT applications, TCO moieties are usually linked to mAb lysine residues, while Tz probes are attached to a macrocycle chelator via polyethylene glycol (PEG) linkers (Fig. 1B/C).

In 2010, Rossin et al. have first demonstrated the proof of concept of IEDDA in living systems, via SPECT-CT imaging using CC49 anti-TAG72 mAb (bearing ≈ 7 TCO/mAb), and an [^{111}In]In-DOTA-Tz probe. Thereafter, IEDDA reaction based on TCO/Tz interaction has been extensively applied for either fluorescence assays, SPECT/PET imaging or preclinical therapy studies and has proved to be a powerful tool to specifically target tumors with low background noise and high tumor to non-target organs ratios. Thereby, imaging investigations demonstrated the possibility to use IEDDA to specifically target tumors with low background noise and high tumor to non-target organs ratios [19–24]. In addition, using PRIT instead of RIT for tumor treatment was all the more interesting since radiation doses received by non-targeted organs were significantly lower with PRIT according to dosimetry calculations [25].

To the best of our knowledge, no clinical studies using pretargeting through IEDDA cycloaddition have been undertaken yet, neither for imaging nor for therapy purpose. However, many preclinical studies based on TCO/Tz interaction essentially focused on the optimization of the Tz moiety and its linker to improve in vivo reaction kinetic and Tz-based radioligand stability in biological media (Fig. 1B) [26,27]. Concerning the TCO moiety, the first study led by Robillard et al. also used a PEGylated linker (e.g. PEG12) [19], PEGylation being a well-known process to reduce the lipophilicity and immunogenicity of immunoconjugates while increasing their blood half-lives [28]. But moving TCO groups away from the mAb

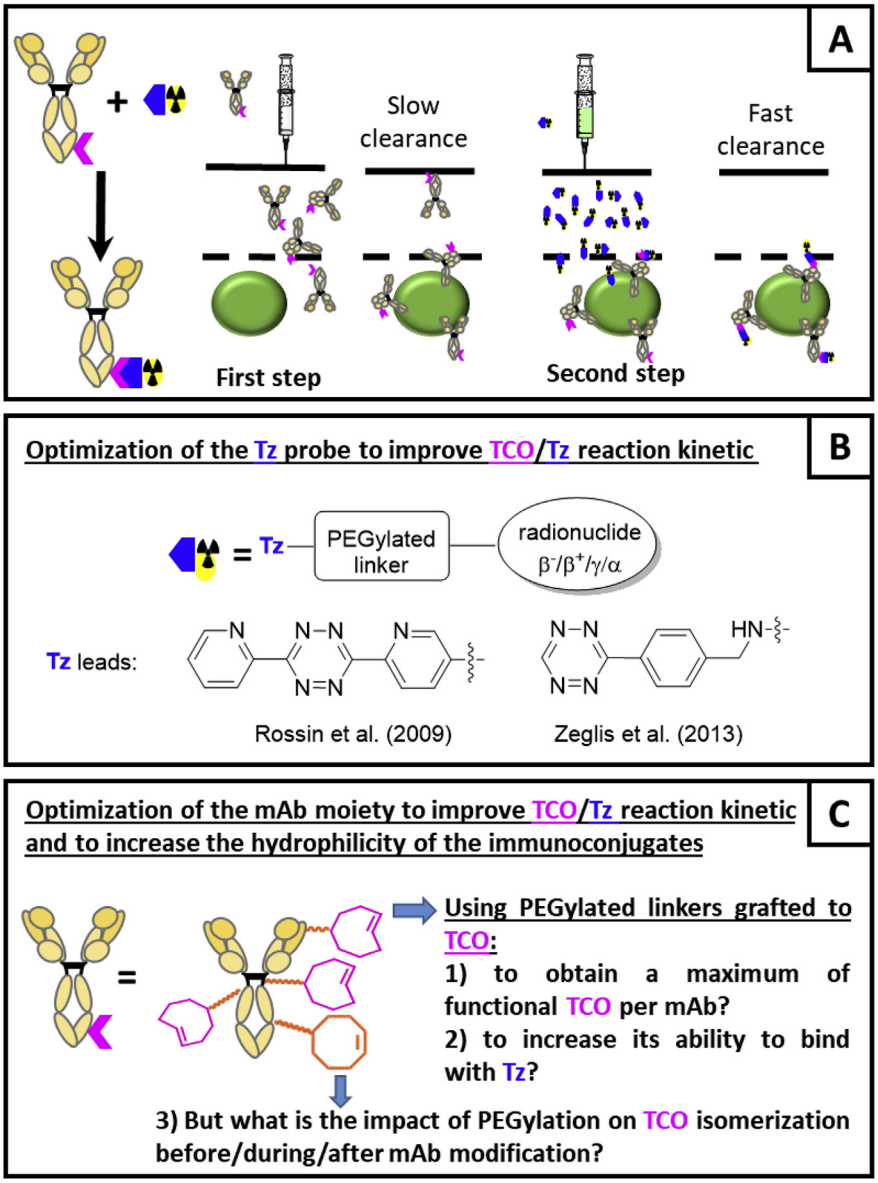

Fig. 1. Principle of the pretargeting strategy (A) and major checkpoints to optimize the TCO/Tz IEDDA cycloaddition (B–C).

surface exposed them to serum protein bound copper (II) (e.g. transcuprein, mouse serum albumin, ceruloplasmin) or thiol derivatives, thus increasing TCO isomerization into its unreactive cis-cyclooctene (CCO) isomer. Others authors have also developed TCOs with exo- or endocyclic heteroatoms. Not only does heteroatom incorporation increase hydrophilicity but it also preserves (or even increases) the reactivity of the cyclic dienophiles [29].

The pioneering teams in the development of the IEDDA system, namely Robillard and Zeglis groups, obtained excellent in vivo results without PEGylated linker between TCO groups and their mAbs (Fig. 1C) [30–32]. We also demonstrated, using fluorescent Tz probes, that PEGylated mAb-TCO were less reactive towards Tz than non-PEGylated mAb-TCO, whatever the length of the linker (e.g. PEG4 and PEG12), either in vitro or in vivo [33,34]. However, Cook et al. recently described the evaluation of a novel bifunctional PEGylated dendrimeric TCO for in vivo PET imaging, resulting in a two-fold improvement of the absolute tumoral uptake [35]. We thereby wondered if one pitfall of the IEDDA system for further clinical application was not the TCO group itself. The purpose of the present study was to determine which critical step(s) could induce TCO isomerization: (i) the introduction of the PEGylated linker during the synthesis of PEGylated TCO derivatives; (ii) the grafting process of TCO derivatives (PEGylated or not) on the mAb; (iii) and/or in vitro and in vivo instability of the mAb-TCO immunoconjugates (either PEGylated or not). To answer these three questions, we first systematically checked the isomerization rate of TCO during all chemical syntheses by analytical HPLC prior to mAb functionalization. However, TCO/CCO conversion can no longer be accurately quantified by analytical HPLC once mAbs were functionalized. Subsequently, we first quantified TCO/Tz interaction by SDS-PAGE-gel electrophoresis, by reacting commercially available fluorescent Tz probes (Tz-Cy3 and Tz-5-FAM) with Ts29.2 mAb conjugates bearing both three different PEG lengths (PEG0, PEG4 and PEG12) and three different TCO/CCO isomeric ratios (90/10; 50/50; 10/90). We then assessed the influence of TCO/CCO isomeric purity by immunofluorescence assays, on HT29 colorectal cell line expressing tetraspanin 8 (TSPAN8) antigen, using the corresponding modified Ts29.2 mAb. The impact of both PEGylation and TCO isomeric purity on mAb-PEG$_x$-TCO stability (x = 0, 4 and 12) were finally evaluated by SDS-PAGE gel electrophoresis monitoring after prior incubation of the different immunoconjugates at 37 °C in PBS or plasma.

2. Results

2.1. Synthesis of pretargeting PEGylated components

The synthesis of PEGylated TCO derivatives started with the photochemical conversion of the commercially available (Z)-cyclooct-4-enol (CCO) into (E)-cyclooct-4-enol (TCO) (Scheme 1).

We succeeded in obtaining TCO with highly reproducible purity rate (e.g. 100/0 TCO/CCO ratio) compared to a 70/30 ratio value previously described by Rossin and co-workers (Fig. S1, **A-B**) [21,36]. A one-pot two-step procedure was first applied to obtain pure **TCO-NHS** and **CCO**–**NHS** compounds. Unfortunately, this synthesis was not as reproducible as expected: most of crude **TCO-NHS** batches usually contained **CCO**–**NHS** isomer in various proportions (up to 22%) with more or less impurities (Fig. S1 C-D). Moreover, conventional chromatographic separation of **TCO-NHS** from **CCO**–**NHS** isomers on normal phase is complex due to their similar polarity. To minimize TCO isomerization, we first tried to perform direct **CCO**–**NHS** irradiation into **TCO-NHS** based on a process recently developed by Bormans and co-workers [37]. Unfortunately, this reaction led only to **TCO (2)** probably due to the photochemical cleavage of the carbamate bond (Fig. S2). Finally, we

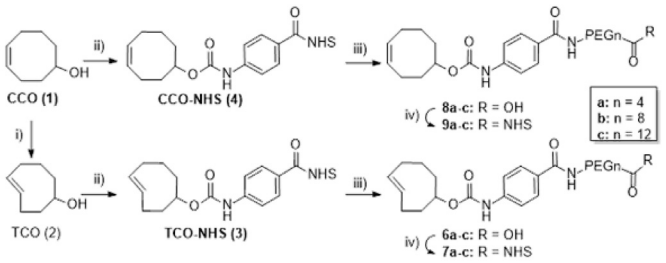

[a]Reactants and conditions: i) h_ν (254 nm, methyl benzoic acid; ii) a) 2,5-dioxopyrrolidin-1-yl 4-aminobenzoic acid, triphosgene; b) TCO or CCO; iii) appropriate $NH_2PEG_xCO_2H$ derivatives **5a-c**, Et_3N; iv) DSC, cat. DMAP.

Scheme 1. TCO derivative syntheses with high TCO/CCO ratio.

focused on the purification of the crude **TCO-NHS** obtained in the first attempt. An original purification process on $AgNO_3$-impregnated silica gel was developed allowing to successively elute **CCO**–**NHS** and impurities with ethyl acetate (control by TLC and HPLC) while **TCO-NHS** was selectively retained by $AgNO_3$. Then, **TCO-NHS** was eluted with a mixture of ethyl acetate/triethylamine (80/20, v/v), leading to a 100% isomeric purity of compound **TCO-NHS**. This original quick and inexpensive method, based on the synthetic procedure to obtain TCO from CCO, allowed to obtain **TCO-NHS** with a 100/0 TCO/CCO ratio in a reproducible manner (Fig. S3) [15,34]. Thereafter, to obtain PEGylated TCO derivatives **7a-c**, we investigated several synthesis methodologies to access PEGylated amino acid precursors $NH_2PEG_xCO_2H$ **5a-c** (Scheme 1). These different strategies are explained in the supporting information (Figs. S4–S7). We finally set an original process for the synthesis of the PEGylated amino acid linkers **5a-c** from the corresponding N_3PEG_xOH involving Jones oxidation of silyl ethers **s9a-c** as key step (Scheme 2).

The PEGylated TCO-derivative **6a** was then obtained by coupling **TCO-NHS** with the PEGylated amino acid linker **5a**, but with the concomitant formation of its PEGylated CCO derivative **8a** and traces of **TCO-NHS**. Attempts to isolate **6a** all proved to be unsuccessful and systematically led to an increased isomerization rate with poor recovery of the desired product regardless the purification method used (washing protocols, purification by normal, reversed phase or $AgNO_3$-silica gel flash chromatography). Therefore, once the starting **TCO-NHS** was almost totally consumed (HPLC monitoring), the crude mixture had to be directly engaged in the following step, using DSC (3 eq.) and catalytic DMAP (0.2 eq.) as optimal experimental conditions, to afford the corresponding activated ester **7a** with an overall yield of 66% and 94% isomeric purity (Fig. S8).

This one-pot two-step method applied to **5a-c** led to **7a-c** with yields ranging from 31 to 67% and with low TCO isomerization after purification by preparative RP-HPLC followed by freeze-drying (Scheme 1; Table 1, **S1** and **S2**).

Using these experimental conditions afforded **7a-c** with TCO/CCO ratio superior to 90/10. $CCOPEG_xCO_2H$ **8a-c** and $CCOPEG_xNHS$ **9a-c** were prepared as reference compounds to control the TCO isomerization rate to CCO by analytical HPLC monitoring during the synthesis of compounds **7a-c** (Fig. S9). All our TCO- and CCO-PEG_xNHS proved to be stable and did not isomerize when conserved at −20 °C as stock solutions in acetonitrile for at least one year.

2.2. Antibody functionalization

Biological experiments were then performed with Ts29.2-based immunoconjugates directed against tetraspanin 8 antigen. The

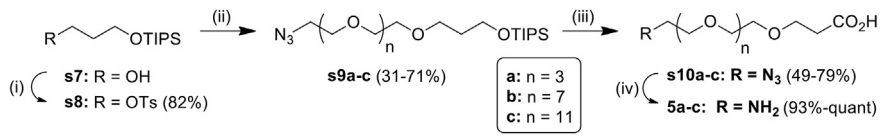

[a]**Reagents and conditions:** (i) TsCl, DMAP, NEt_3, dichloromethane, rt; (ii) *Method A:* appropriate compound $N_3PEGxOH$, THF, NaH 60%, then **s8**; *Method B*: **s7**,THF, NaH 60%, then appropriate compound $N_3PEGxOH$; (iii) H_2SO_4, CrO_3, acetone, rt; (iv) H_2, Pd/C 10%, ethanol, rt; (v) TFA, CH_2Cl_2, rt, quantitative.

Scheme 2. Synthesis of compounds $NH_2PEG_xCO_2H$ **5a-c** (x = 4, 8 and 12).

Table 1
Synthesis of compounds $TCOPEG_xCONHS$ **7a-c** (x = 4, 8 and 12).

Reactant	Step 1 (5a-c into 6a-c)		Step 2 (6a-c into 7a-c)		Yield (%)
	Product	TCO/CCO ratio	Product	TCO/CCO ratio	
5a	**6a**	100/0	**7a**	94/6	66
5b	**6b**	100/0	**7b**	99/1	31
5c	**6c**	94/6	**7c**	93/7	67

in vitro and in vivo proof-of-concepts of IEDDA pretargeting for fluorescence imaging of colorectal cancer and peritoneal carcinomatosis were recently published by our team [32,33]. Different amounts of CCO derivatives (e.g; CCO–NHS **4** or **9a** or **9c**) were added to the TCO derivatives (e.g; TCO-NHS **3** or **7a** or **7c**, respectively) adducts so as to obtain fixed TCO/CCO ratios (e.g. 90/10, 50/50 and 10/90). Control of TCO/CCO ratios was systematically performed using analytical HPLC both before and after adding CCO isomers (Scheme 3; Fig. S10, **S11** and **S12**).

Ts29.2 was then modified by addition of the appropriate TCO-NHS **3**/CCO–NHS **4** mixture (ratio 1, 2 or 3) to afford the expected modified Ts29-2-TCO immunoconjugates, namely **Ts29.2(PEG_0)@1a**, **Ts29.2(PEG_0)@2a** or **Ts29–2(PEG_0)@3a**. Similar procedures were performed to produce **Ts29.2(PEG_4)@1b** to **Ts29.2(PEG_{12})@3c** by addition of the appropriate mixture of **7a/9a** or **7c/9c** for ratios 1–3 (Scheme 3). The mean number of TCO-CCO moieties grafted per mAb ranged from 7.6 to 7.9 for **Ts29.2(PEG_0)@1a-Ts29.2(PEG_0)@3a** and from 4.1 to 4.9 for both **Ts29.2(PEG_4)@1b-Ts29.2(PEG_4)@3b**, **Ts29.2(PEG_{12})@1c-Ts29.2(PEG_{12})@3c** (n = 3) (Table S3).

2.3. Immunofluorescence assays on HT29 cells

Assays were made with all Ts29.2-PEG_x-TCO ± CCO (x = 4, 8 and 12) (e.g. **Ts29.2(PEG_{12})@1a** to **Ts29.2(PEG_0)@3c,** Fig. 2) as described in supporting information.

Whatever the PEG linker used (PEG0, PEG4 or PEG12), we observed, as expected, a strong decrease of the fluorescence intensity located at the cell membrane in correlation with the decrease of the TCO proportion. As expected, the mean fluorescence intensity, reflecting the TCO/Tz ligation, was higher with TCO/CCO ratio of 90/10 whatever the length of PEG chain but became weaker as the amount of CCO increases (e.g. TCO/CCO isomeric purity ratio decreases) (Fig. 3). Quantification of the mean fluorescence intensity confirmed this tendency for all PEG linkers.

It was observed that the decrease of the mean fluorescence intensity is lower with PEG0 than PEG4 and PEG12 for all the corresponding isomeric ratios (Figs. 2 and 3). The presence of PEGylated linkers was suspected to induce a faster TCO isomerization. Nevertheless, we can notice that for a 90/10 TCO/CCO ratio, a higher mean fluorescence signal was obtained with PEG4. Then, the influence of PEGylation on Ts29.2-PEG_x-TCO/CCO stability over time was assessed using SDS-PAGE gel electrophoresis after prior incubations of all immunoconjugates either in D-PBS (control, Fig. 4) or in murine plasma, at 37 °C for 1–24 h (Fig. 5).

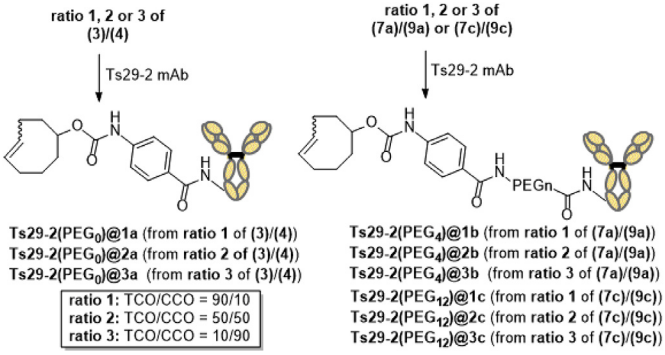

Scheme 3. Ts29-2 functionalization with mixtures of TCO- and CCO–NHS esters.

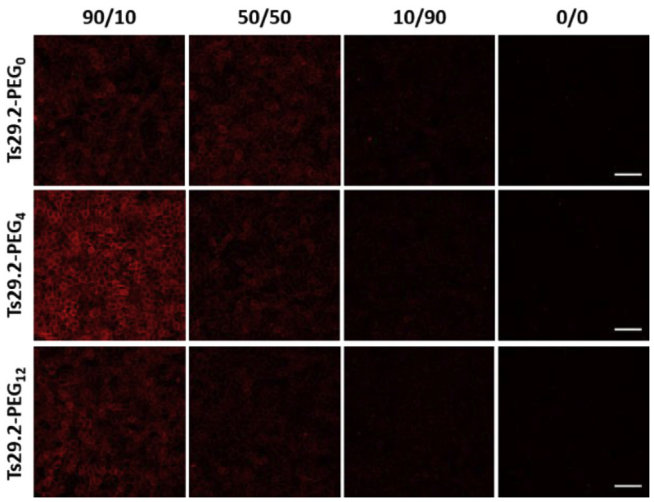

Fig. 2. Assessment of the interaction between Ts29.2-TCO/CCO and Tz-Cy3 through immunofluorescence assays.

In D-PBS at 37 °C, a progressive decrease of fluorescence intensity was observed as expected, as the CCO isomeric rate increased whatever the PEG length. With PEG0/PEG4 immunoconjugates prepared from ratio 1 (e.g. TCO/CCO 90/10), the fluorescence intensity, reflecting the interaction between Ts29.2-PEG_x-TCO and the tetrazine probe, slightly decreased in the first hours then remained relatively stable between 5 h and 24 h. However, a significant decrease was observed for ratios 2 and 3 regardless the PEG length over the 24 h incubation period. Regarding PEG12 derivatives, the fluorescence intensity decreased continuously over 24 h, whatever the starting ratio. We have checked that the incubation between immunoconjugates and Tz-5-FAM before gel electrophoresis gave similar results compared to incubation of the gel in Tz bath after migration (Fig. S15).

Concerning the stability of the three immunoconjugates

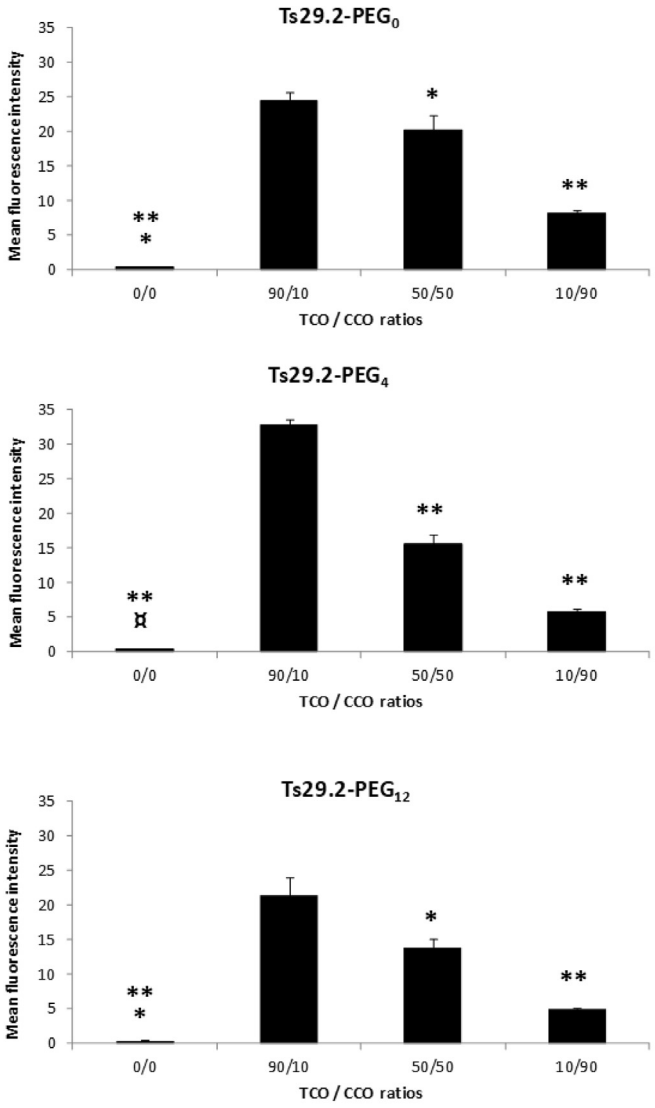

Fig. 3. Quantification of the mean fluorescence intensity localized on the cell membrane using ImageJ software. *P < 0.05: 0/0 vs 10/90 and 50/50 vs 90/10; * P < 0.001: 0/0 vs 10/90, ** P < 0.0001: 0/0 vs 90/10 and 50/50, 10/90 vs 50/50 and 90/10, and 50/50 vs 90/10. (n = 3 independent experiments).

incubated at 37 °C in murine plasma, for each PEG length and whatever the TCO/CCO ratio, fluorescence intensity significantly decreased within 5 h of incubation compared to D-PBS. However, from 5 h to 24 h, there were few differences except for PEG12 immunoconjugates because there are no reactivity after 5h of contact in plasma. We found that the higher the percentage of CCO before mAb grafting, the faster the fluorescence intensity decreased, and consequently, the TCO/Tz interaction. Thereby, after 5 h of incubation in plasma, the presence of a PEGylated linker seemed to dramatically increase TCO to CCO isomerization. Indeed, for PEG12, a total loss of fluorescence intensity occurred within 5 h, compared to 80% and 90% loss for PEG0 and PEG4 conjugates respectively. These results suggested that introducing a long PEG linker on mAb could be highly detrimental for in vivo IEDDA cycloaddition between TCO and Tz as TCO groups would be more easily exposed to plasma proteins. Conversely, **Ts29.2(PEG0)@1a-Ts29.2(PEG0)@3a** conjugates would be potentially more stable in vivo, which could be explained by the proximity of TCO from the mAb surface.

3. Discussion

While immunopretargeting is not a recent approach, the development of bioorthogonal chemistry has challenged this concept by favouring dosimetry through the specific delivery of therapeutic radiations to solid tumors while reducing the non-specific uptake in non-targeted tissues. The most promising method is based on the trans-cyclooctene (TCO)/tetrazine (Tz) cycloaddition (IEDDA) which has already been the subject of several publications for both optical imaging, PET, SPECT and radioimmunotherapy (β^- and α) [17,19,24,30,32,34,38–40]. Moreover, a recent review exhaustively identified 25 PubMed articles reporting preclinical imaging and five therapy studies with full mAbs as targeting vectors, since its first application in 2010 [7]. However, to the best of our knowledge, no clinical trials have yet been undertaken with this concept, neither for imaging nor for therapy purpose, despite these very promising in vivo results reported in different models of cancer. This is quite surprising considering that bioorthogonal chemistries, previously difficult to synthesize, are nowadays commercially available. The Achilles' heel of the TCO/Tz tandem thereby seems to rely on the stability of the TCO group itself. Indeed, if TCO isomerizes into its less-reactive form cis-cyclooctene (CCO), the ligation with tetrazine becomes very slow. To counteract this known isomerization issue, assessments of either modifications on TCO structure [5,41] or increasing of the number of TCO moieties conjugated on mAbs via the addition of dendritic TCO were performed and led to an improvement of TCO stability, but also highlighted that optimizations are still needed. Other interesting strategies consisting in the reaction of Tz moieties with constrained alkyne derivatives -which would prevent the isomerization-are also under investigation but the ligation kinetic is less efficient [5].

Despite potential isomerization, the bioconjugation of TCO with antibodies remains an interesting therapeutic option for the potential treatment of many cancers. We here thereby decided to focus on the optimization of TCO derivatives and to investigate the process of TCO/CCO isomerization supposedly occurring:(i) during the synthesis of PEGylated TCO derivatives; (ii) and/or during the grafting process of (PEGylated or not) TCO derivatives on the mAb; (iii) and/or during in vitro and/or in vivo experiments.

The synthesis of PEGylated amino acid derivatives -not always commercially available in Europe-is often expensive when PEG are longer than four oligomeric units and not easy to synthesize. We therefore developed several synthetic methods to obtain these different PEGylated amino acids which could finally be extended to different PEGylated derivatives longer than 12 oligomeric units.

During the synthesis of PEGylated TCO derivatives, we monitored the isomerization of TCO by analytical HPLC at each step. We have thus demonstrated that the precursor **TCO-NHS** can be easily and efficiently obtained with 100% of isomeric purity via the use of an $AgNO_3$/silica cartridge. In addition, the optimized TCO-NHS precursor was also employed in our team for the conjugation of anti-CEA 35A7 mAb [33] as well as for clinical approved mAbs such as Rituximab, Cetuximab and Panitunimab (data not shown).

This is quite interesting as most studies recommend to directly conjugate TCO to the mAb, without any PEG linkers, in order to improve the in vivo stability induced by the shielding effect of the mAb against Cu-containing serum proteins supposedly isomerizing TCO into non-reactive CCO [31]. This optimization could be helpful to a wide variety of new applications, such as the recently developed "PeptoBrush concept", which allow a higher TCO-loading on an biodegradable co-polymer showing EPR-mediated tumor accumulation than on antibodies for which it is generally advised to not exceed 4 grafted entities (2<DAR<5) or the dendrimer-bearing TCO conjugated site-specifically to the Fc fragment of mAb

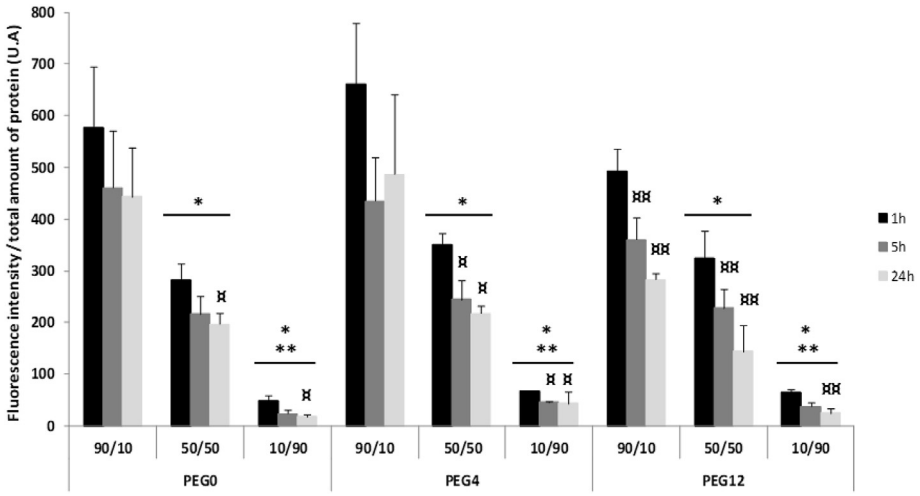

Fig. 4. Influence of the amount of CCO in the reaction medium before Ts29.2 grafting on both Ts29.2-PEG$_x$-TCO stability in D-PBS and interaction with Tz-5-FAM. * P < 0.05: 50/50 vs 90/10 and 10/90 vs 50/50; ** p < 0.001: 10/90 vs 90/10; ¤ p < 0.05: 24 h vs 1 h, 5 h vs 1 h, 24 h vs 5 h ** p < 0.001: 5 h and 24 h vs 1 h (n ≥ 3 independent experiments).

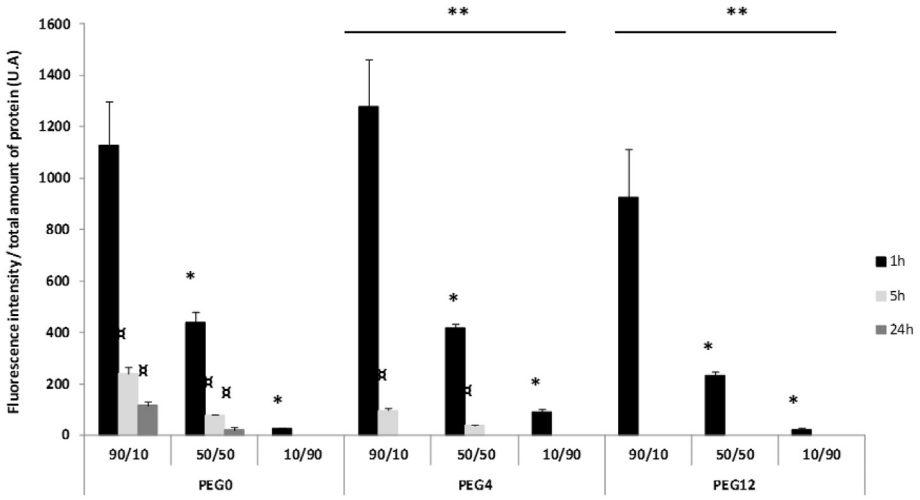

Fig. 5. Influence of the amount of CCO in the reaction medium before Ts29.2 grafting on both Ts29.2-PEG$_x$-TCO stability in mice plasma diluted in 50% D-PBS and interaction with Tz-5-FAM. *P < 0.0001: 50/50 vs 90/10, 10/90 vs 90/10 and 10/90 vs 50/50; **p < 0.001: PEG4 vs PEG0, PEG12 vs PEG0 and PEG12 vs PEG4; ¤ p < 0.0001: 24h vs 1 h, 24 h vs 5 h and 5 h vs 1 h (n ≥ 3 independent experiments).

[5,35,42–45]. Indeed, the concept of "high TCO loading" undoubtedly compensates for the non-reactivity of isomerized TCO by increasing the possibility of ligation towards Tz. Moreover, ensuring that **TCO-NHS** precursors are 100% isomerically pure before functionalizing the co-polymer of the dendritic structure would be an additional advantage to reduce the inactivation of moieties. With this in mind, our method for controlling TCO isomerization rate below 10% with PEGylated linkers prior to mAb grafting makes sense. In our experiments no isomerization was observed during the conjugation of TCO derivatives (PEGylated or not) on the mAb (Fig. 3). We can even note that 90/10 and 50/50 ratios have given almost similar results with no PEGylated spacers in D-PBS at 37 °C. From 5 h to 24 h of incubation in D-PBS, there are few differences except for the PEG12 conjugate. The results highlight that the control of isomerization rate prior to antibody conjugation is an important issue and could be a helpful tool for further investigations to increase active TCO at the tumour level and slowing its possible in vivo isomerization with or without PEGylated spacers.

Since we are able to optimize and control the isomerization before and during the modification of the antibody, we then questioned about our third hypothesis concerning the in vivo deactivation of TCO. Within the immunoconjugate assays, for each PEG length and whatever the TCO/CCO ratio we observed that fluorescence intensity slightly decreased over 5 h of incubation in plasma (Fig. 5). In addition, the higher the percentage of CCO before the functionalization of the mAb, the lower the fluorescence intensity. After 5 h of incubation in this media, the presence of a PEGylated linker dramatically raised the isomerization of TCO into CCO. Once again, we observed that the higher the percentage of CCO before mAb's functionalization the lower the fluorescence intensity. The present study is consistent with our previous work, confirming that **Ts29.2(PEG0)@1a** is the most appropriate conjugate for further PRIT studies, and brings new information about the behaviour of Ts29.2 immunoconjugates in plasma, hence reflecting their potential behaviour in vivo [33].

In vitro assays using Ts29-PEG$_x$-TCO conjugates confirmed that a fast TCO isomerization was correlated to an increased length of PEGylated linkers, and more notably in murine plasma (superior to 90% for PEGylated conjugates after only 5 h of incubation). Despite

this surprising results obtained in vitro after 5 h, we observed in vivo IEDDA ligation 24 h following injection of mAb-TCO with fluorescent Tz or [^{111}In]In-DOTA-Tz probes [33,34].

Moreover, several in vivo PRIT investigations of using IEDDA cycloaddition reported interactions between mAbs-TCO and Tz injected 48 or 72 h after the immunoconjugate [34,44]. The authors demonstrated that the interaction is nevertheless weaker than the one observed at 24 h (i.e. 11 and 13 vs 21 %IA/g, respectively) [44]. For present results, we can hypothesize that the incubation of the mAbs TCO in this ex vivo condition did not reflect entirely the in vivo situation: plasma is not full blood, absence of fluid mechanism, ratio of mAbs-TCO/plasmatic protein was different (in vivo 50 μg mAbs TCO diluted in 1.3 mL of blood and in vitro 5 μg diluted in 50 μL of plasma). Additionally, potential mAb-TCO degradation cannot be checked with this approach. Our in vitro experiments were then performed under drastic conditions to demonstrate the interest of controlling the isomerization rate before conjugation in order to maximize the possibility of reaction towards Tz in vivo. The results obtained cannot be considered as the reflect of in vivo processes of TCO isomerization. This demonstrated a loss of in vivo TCO/Tz interaction over time, thereby corroborating our in vitro observations. In view of the recent results of Zeglis [44], this is not only due to isomerization but also to other mechanisms that will have to be highlighted in order to clinically transfer this concept of pretargeting as soon as possible.

4. Conclusion

In conclusion, we here developed an efficient method to synthesize (PEGylated)TCO derivatives with high isomeric purity and monitoring the TCO:CCO ratio via HPLC before the conjugation of mAbs. Our original method is easy to use, fast and highly reproducible either for direct TCO activated ester precursors or for the conjugation of PEGylated TCO derivatives. The $AgNO_3$ impregnated silica gel allows obtaining precursor **3** with a 100% of isomeric purity while the optimized one-pot two-step synthesis process of compounds **7a-c**, **8a-c** and **9a-c**, resulting in excellent TCO isomeric purity of at least 94% before mAbs conjugation. In vitro assays using Ts29-PEG$_x$-TCO conjugates confirmed thereafter that a fast TCO deactivation was correlated to an increased length of PEGylated linkers, and more notably in murine plasma (superior to 90% for PEGylated conjugates after only 5 h of incubation).

This work represents a helpful tool for further investigations on TCO/Tz reaction for PRIT experiments by allowing controlling the TCO isomerization rate to obtain a TCO prosthetic group with a TCO:CCO ratio as close as possible to 100:0 before mAb conjugation. The process decried herein can be applied to a wide range of mAbs thereby arousing a great interest for further SPECT/PET imaging and/or PRIT applications using IEDDA cycloaddition, especially for considering the GMP transfer of IEDDA bioorthogonal chemistry to the clinic.

5. Experimental section

5.1. Materials for chemical syntheses

Unless otherwise mentioned, all manipulations were performed under argon atmosphere; all reagents were purchased from the following commercial suppliers: Sigma-Aldrich, Acros Organics, Carlo Erba, TCI Europa, Alfa Aesar. Anhydrous DMF, anhydrous triethylamine and anhydrous pyridine were purchased from Acros Organics. THF was dried over a Pure Solv™ Micro Solvent Purification System (Sigma-Aldrich) equipped with an alumina column. Dichloromethane was distilled over calcium hydride. Reaction progresses were monitored by thin layer chromatography (TLC) using 60 F254 or alumina gel 60A + F254 plates and visualized with UV light (UV lamp Fisher Bioblock Scientific, 365 nm or 254 nm), dragendorff revelator (1.6 g of bismuth (III) nitrate for 100 mL of glacial acetic acid/H_2O (1/4, v/v), $KMnO_4$ (1.5 g for 100 mL of water) or phosphomolybdic acid (8 g for 200 mL of ethanol). Uncorrected melting points (mp) were measured on an IA9100 Digital Melting Point Apparatus. Purifications by column chromatography were performed on silica gel (Chromagel 60 ACC, 40–63 μm, Carlo Erba Reagents). Purifications by preparative reversed-phase HPLC were conducted on a Combiflash EZ prep system (Teledyne Isco) with a RP-18 column (250 mm × 20 mm, pores 100 Å, particles 5 μM). All the PEG derivatives used in synthesis were systematically dried by co-evaporation with anhydrous toluene twice and flushed with argon before use, unless otherwise stated. HT29 cell line, a colon adenocarcinoma cell line expressing TSPAN8, and the non-internalizing murine monoclonal antibody (mAb) directed against tetraspanine 8, Ts29.2 (IgG2b), were provided by Dr. C. Boucheix (Inserm, Villejuif, France). Cells were cultured in Dulbecco's Modified Eagle F12 Medium supplemented with 10% fetal serum, 1% penicillin/streptomycin, 1% geneticin, 1% hygromycin at 37 °C with 5% CO_2 in humidified environment. For the different experiments, two fluorescent Tz probes were purchased at JenaBioscience (Germany), namely 3-(p-benzylamino)-1.2.4.5-tetrazine-5-Fluorescein (Tz-5-FAM, absorbance/emission wavelengths 492/517 nm, molecular weight (MW) 545.50 g/mol) and 3-(p-benzylamino)-1.2.4.5-tetrazine-cyanine3 (Tz-Cy3, absorbance/emission wavelengths 550/570 nm, MW 908.07 g/mol). Those different fluorophores do not alter the ability of Tz to bind TCO moieties due to the high affinity and specificity of Tz for TCO and due to their ability as organic dyes to not interfere with biological functions. In addition, in a same experiment, we always compared mAb immunoconjugates using the same fluorescent Tz probe -e.g the most adapted to obtain significant signal detection according to the laser capacity of the device used-in order to avoid introduction of any bias. Signal observation was made using a confocal imager (Leica SPE, ICCF platform, Clermont-Ferrand, France). Statistical analysis was performed using XLSTAT 2012 software. Continuous data were expressed with the mean and standard deviation (SEM). To compare continuous values of the different modified antibodies, a one-way ANOVA or two-paired Student T-test were used. We considered $p < 0.05$ statistically significant. Native monoclonal antibody Ts29.2 was solvent-exchanged and concentrated on Amicon Ultra-4 centrifugal filter units (50 kDa MW cut-off) using D-PBS (Gibco) to reach a final concentration between 5 and 10 μg/μL before use, whereas TCO-grafted antibodies were purified on Zeba desalting spin columns (40 kDa MW cut-off, 0.5 mL, ThermoFisher scientific). Concentrations of mAb-TCO conjugates were determined with a MultiskanTM go spectrophotometer (ThermoFisher Scientific) at 280 nm while the mean number of TCO grafted by mAb was determined by MALDI-ToF mass spectrometry.

Syntheses. The synthesis of TCO **(2)**, TCO-NHS **(3)**, CCO–NHS **(5)** and all others syntheses were developed in the supporting information.

5.1.1. General procedure for syntheses of compounds (7a-c) and (9a-c)

To a solution of **TCO-NHS (3)** or **CCO–NHS (4)** (approx. 20–30 mg, 1 eq.) in anhydrous dichloromethane (1 mL) were successively added anhydrous triethylamine (10 eq.) and a solution of the appropriate PEGylated aminoacid (5a-c) (1.5 eq.) in anhydrous dichloromethane (1.5 mL) at room temperature and under argon atmosphere. After completion of the reaction (HPLC monitoring), DMAP (0.2 eq.) and N,N′-disuccinimidyl carbonate (DSC) (3 eq.) were added. The resulting reaction mixture was stirred for 1 h, then successively washed with a hydrochloric acid solution (0.5 M)

(2.5 mL), water (3 x 4 mL) and brine (6 mL), dried over $MgSO_4$, filtered and evaporated under reduced pressure to afford the desired crude product as a pale yellow lacquer. Then, the crude product was purified by preparative RP-HPLC with a water/acetonitrile gradient, namely 50/50 to 20/80 over 15 min then 20/80 to 0/100 over 5 min, providing after freeze-drying the desired activated ester. Stock solutions of **TCO-NHS (3)**, **CCO**−**NHS (4)**, $TCOPEG_xNHS$ esters **(7a-c)** and $CCOPEG_xNHS$ esters **(9a-c)** in DMSO for antibody conjugation were prepared and stored at −20 °C in the dark and proved to be stable for at least a year.

5.1.1.1. (E)-2,5-dioxopyrrolidin-1-yl 1-(4-(((cyclooct-4-en-1-yloxy) carbonyl)amino)phenyl)-1-oxo-5,8,11,14-tetraoxa-2-azaheptadecan-17-oate (7a). General procedure using **TCO-NHS (3)** (20 mg, 0.052 mmol, 1 eq.), anhydrous triethylamine (72 μL, 0.52 mmol, 10 eq.) and **5a** (20.7 mg, 0.078 mmol), followed 4 h later by addition of DMAP (1.3 mg, 0.01 mmol) and DSC (42 mg, 0.156 mmol) (HPLC monitoring) afforded compound **7a** as a colorless oil (21.7 mg, 0.034 mmol, 66%). HPLC: TR = 7.21 min (λ_{max} = 265 nm), purity = 99%, TCO/CCO = 94/6. Revelator: UV and phosphomolybdic acid. ^{1}H NMR (500 MHz, $CDCl_3$) δ 1.56−2.40 (m, 10H, H2'',H3'', H4'',H7'',H8''), 2.81 (s, 4H, Hb), 2.84 (t, *J* = 6.5 Hz, 2H, H2), 3,59-3,66 (m, 16 H, CH_2−O), 3.79 (t, *J* = 6.5 Hz, 2H, H3), 4.45 (m, 1H, H1''), 5.47−5.65 (m, 2H, H5'', H6''), 6,85 (brs, 2H, NH), 7.42 (d, *J* = 9.0 Hz, 2H, H2′, H6′), 7.75 (d, *J* = 9.0 Hz, 2H, H3′, H5'); ^{13}C NMR (125 MHz, $CDCl_3$) δ 25.6, 31.0, 32.2, 32.5, 34.2, 38.6, 39.8, 41.1, 65.7, 69.8, 70.3, 70.5 (2C), 70.6 (2C), 70.7, 81.5, 117.7, 128.2, 129.0, 133.1, 134.9, 141.1, 152.8, 166.7, 166.9, 169.0; HRMS (ESI+) *m/z* calculated from $C_{31}H_{44}O_{11}N_3$ 634.2970 $[M+H]^+$; found 634.2980.

5.1.1.2. (E)-2,5-dioxopyrrolidin-1-yl 1-(4-(((cyclooct-4-en-1-yloxy) carbonyl)amino)phenyl)-1-oxo-5,8,11,14,17,20,23,26-octaoxa-2-azanonacosan-29-oate (7b). General procedure using **TCO-NHS (3)** (21 mg, 0.054 mmol), anhydrous triethylamine (75 μL, 0.54 mmol) and **5b** (35.8 mg, 0.081 mmol), followed 21 h later by addition of DMAP (1.3 mg, 0.010 mmol) and DSC (42 mg, 0.156 mmol) (HPLC monitoring) afforded compound **7b** as a colorless oil (13,6 mg, 0.017 mmol, 31%). HPLC: TR = 6.99 min (λ_{max} = 265 nm), purity = 97%, TCO/CCO = 99/1. Revelator: UV and phosphomolybdic acid. ^{1}H NMR (500 MHz, $CDCl_3$) δ 1.56−2.40 (m, 10H, H2'',H3'', H4'',H7'',H8''), 2.80 (s, 4H, Hb), 2.86 (m, 2H, H2), 3.55−3.67 (m, 16 H, CH2−O), 3.81 (m, 2H, H3), 4.44 (m, 1H, H1''), 5.47−5.63 (m, 2H, H5'', H6''), 6.92 (brs, 1H, NH), 7.18 (brs, 1H, NH), 7.43 (d, *J* = 9.0 Hz, 2H, H2′, H6′), 7.75 (d, *J* = 9.0 Hz, 2H, H3′, H5'). ^{13}C NMR (125 MHz, $CDCl_3$) δ 25.6, 31.0, 32.2, 32.5, 34.2, 38.6, 39.8, 41.1, 65.7, 69.9, 70.2, 70.5 x 2, 70.6, 70.7 x 2, 81.3, 117.7, 128.2, 128.9, 133.0, 134.9, 141.3, 152.9, 166.7, 166.9, 168.9. HRMS (ESI+) *m/z* calculated from $C_{39}H_{60}O_{15}N_3$ 810.4019 $[M+H]^+$; found 810.4023.

5.1.1.3. (E)-2,5-dioxopyrrolidin-1-yl 1-(4-(((cyclooct-4-en-1-yloxy) carbonyl)amino)phenyl)-1-oxo-5,8,11,14,17,20,23,26,29,32,35,38-dodecaoxa-2-azahentetracontan-41-oate (7c). [31] General procedure using **TCO-NHS (3)** (22 mg, 0.057 mmol, 1 eq.), anhydrous triethylamine (79 μL, 0.57 mmol, 10 eq.) and **5c** (52.8 mg, 0.086 mmol, 1.5 eq.), followed 21 h after by addition of DMAP (1.4 mg, 0.011 mmol) and DSC (46.1 mg, 0.171 mmol) (HPLC monitoring) afforded compound **7c** as a colorless oil (37.6 mg, 0.038 mmol, 67%). HPLC: TR = 6.78 min (λ_{max} = 265 nm), purity = 98%, TCO/CCO 93/7. Revelator: UV and phosphomolybdic acid. ^{1}H NMR (500 MHz, $CDCl_3$) δ 1.56−2.40 (m, 10H, H2'',H3'', H4'',H7'',H8''), 2.81 (s, 4H, Hb), 2.84 (m, 2H, H2), 3.58−3.64 (m, 48 H, CH2−O), 3.83 (m, 2H, H3), 4.45 (m, 1H, H1''), 5.49−5.70 (m, 2H, H5'', H6''), 6.92 (brs, 1H, NH), 7.05 (brs, 2H, NH), 7.44 (d, *J* = 9.0 Hz, 2H, H2′, H6′), 7.75 (d, *J* = 9.0 Hz, 2H, H3′, H5'); ^{13}C NMR (125 MHz, $CDCl_3$) δ 25.6, 31.0, 32.2, 32.5, 35.0, 38.6, 39.8, 41.1, 65.7, 69.9, 70.2, 70.5, 70.6 x 2, 70.7, 81.4, 117.7, 128.2, 129.0, 133.1, 134.9, 141.2, 152.8, 166.7, 166.9, 168.9; HRMS (ESI+) *m/z* calculated for $C_{47}H_{76}O_{19}N_3$ 986.5068 $[M+H]^+$; found 986.5064.

5.1.1.4. (Z)-2,5-dioxopyrrolidin-1-yl 1-(4-(((cyclooct-4-en-1-yloxy) carbonyl)amino)phenyl)-1-oxo-5,8,11,14-tetraoxa-2-azaheptadecan-17-oate (9a). General procedure using **CCO**−**NHS (4)** (20 mg, 0.052 mmol, 1 eq.), anhydrous triethylamine (72 μL, 0.52 mmol, 10 eq.) and **5a** (20.7 mg, 0.078 mmol, 1.5 eq.), followed 4 h after by addition of DMAP (1.3 mg, 0.010 mmol) and DSC (42 mg, 0.156 mmol) (HPLC monitoring) afforded compound **9a** as a colorless oil (19.7 mg, 0.031 mmol, 60%). HPLC: TR = 7.67 min (λ_{max} = 265 nm), purity = 98%. Revelator: UV and phosphomolybdic acid. ^{1}H NMR (500 MHz, $CDCl_3$) δ 1.57−2.40 (m, 10H, H2'',H3'', H4'',H7'',H8''), 2.79 (s, 4H, Hb), 2.83 (t, *J* = 6.5 Hz, 2H, H2), 3.58−3.64 (m, 16 H, CH2−O), 3.78 (t, *J* = 6.5 Hz, 2H, H3), 4.83 (m, 1H, H1''), 5.55−5.71 (m, 2H, H5'', H6''), 6.92 (brs, 1H, NH), 6.98 (brs, 1H, NH), 7.42 (d, *J* = 9.0 Hz, 2H, H2′, H6′), 7.74 (d, *J* = 9.0 Hz, 2H, H3′, H5'); ^{13}C NMR (125 MHz, $CDCl_3$) δ 22.3, 24.8, 25.6, 32.1, 33.8, 33.9, 39.8, 65.7, 69.9, 70.2, 70.4, 70.5 x 2, 70.6, 70.7, 77.0, 116.3, 117.7, 128.2, 128.9, 129.5, 129.8, 141.2, 152.9, 166.8, 167.0, 169.1; HRMS (ESI+): *m/z* calculated for $C_{31}H_{44}O_{11}N_3$ 634.2970 $[M+H]^+$; found 634.2966.

5.1.1.5. (Z)-2,5-dioxopyrrolidin-1-yl 1-(4-(((cyclooct-4-en-1-yloxy) carbonyl)amino)phenyl)-1-oxo-5,8,11,14,17,20,23,26-octaoxa-2-azanonacosan-29-oate (9b). General procedure using **CCO**−**NHS (4)** (20 mg, 0.052 mmol), anhydrous triethylamine (72 μL, 0.52 mmol, 10 eq.) and **5b** (34.3 mg, 0.078 mmol, 1.5 eq.), followed 21 h after by addition of DMAP (1.3 mg, 0.010 mmol) and DSC (42 mg, 0.156 mmol) (HPLC monitoring) afforded compound **9b** as a colorless oil (17.1 mg, 0.021 mmol, 41%). HPLC: TR = 7.42 min (λ_{max} = 265 nm), purity = 99%. Revelator: UV and phosphomolybdic acid. ^{1}H NMR (500 MHz, $CDCl_3$) δ 1.55−2.38 (m, 10H, H2'',H3'', H4'',H7'',H8''), 2.80 (s, 4H, Hb), 2.85 (t, J = 6,5 Hz, 2H, H2), 3.56−3.65 (m, 32 H, CH2−O), 3.80 (t, J = 6,5 Hz, 2H, H3), 4.83 (m, 1H, H1''), 5.59−5.71 (m, 2H, H5'', H6''), 6.92 (m, 1H, NH), 7.14 (brs, 1H, NH), 7.44 (d, *J* = 9.0 Hz, 2H, H2′, H6′), 7.75 (d, *J* = 9.0 Hz, 2H, H3′, H5'); ^{13}C NMR (125 MHz, $CDCl_3$) δ 22.3, 24.8, 25.6, 32.2, 34.0, 39.8, 69.9, 70.2, 70.5 x 3, 70.6, 70.7, 77.0, 116.3, 117.8, 128.2, 128.9, 129.5, 129.8, 141.3, 153.0, 166.7, 166.9, 168.9; HRMS (ESI+): *m/z* calculated for $C_{39}H_{60}O_{15}N_3$ 810.4019 $[M+H]^+$; found 810.4015.

5.1.1.6. 2,5-dioxopyrrolidin-1-yl (Z)-1-(4-(((cyclooct-4-en-1-yloxy) carbonyl)amino)phenyl) −41-oxo-4,7,10,13,16,19,22,25,28,31,34,37-dodecaoxa-40-azahentetracontanoate (9c). General procedure using **CCO**−**NHS (4)** (20 mg, 0.052 mmol, 1 eq.), anhydrous triethylamine (72 μL, 0.52 mmol, 10 eq.) and **5c** (48.2 mg, 0.078 mmol, 1.5 eq.), followed 21 h after, DMAP (1.3 mg, 0.010 mmol) and DSC (42 mg, 0.156 mmol) (HPLC monitoring) afforded compound **9c** as a colorless oil (24.7 mg, 0.025 mmol, 48%). HPLC: TR = 7.13 min (λ_{max} = 265 nm), purity = 99%. Revelator: UV and phosphomolybdic acid. ^{1}H NMR (500 MHz, $CDCl_3$) δ 1.58−2.38 (m, 10H, H2'',H3'', H4'',H7'',H8''), 2.80 (s, 4H, Hb), 2.86 (t, *J* = 6.5 Hz, 2H, H2), 3.56−3.62 (m, 48 H, CH2−O), 3.81 (t, *J* = 6.5 Hz, 2H, H3), 4.82 (m, 1H, H1''), 5.61−5.70 (m, 2H, H5'', H6''), 6.83 (m, 1H, NH), 7.20 (brs, 1H, NH), 7.45 (d, *J* = 8.5 Hz, 2H, H2′, H6′), 7.73 (d, *J* = 8.5 Hz, 2H, H3′, H5'); ^{13}C NMR (125 MHz, $CDCl_3$) δ 22.4, 24.7, 25.6, 32.3, 33.6, 33.9, 39.8, 65.8, 69.8, 70.3, 70.6, 70.7, 77.0, 117.9, 128.1, 129.2, 129.5, 129.7, 141.3, 152.9, 166.6, 166.8, 168.7; HRMS (ESI+): *m/z* calculated for $C_{47}H_{76}O_{19}N_3$ 986.5068 $[M+H]^+$; found 986.5075.

5.2. HPLC monitoring

Analyses and monitoring of reactions involving TCO and CCO

derivatives were performed by analytical RP-HPLC on an Agilent 1100 HPLC system using an Agilent Zorbax extend C-18 column (4.6 × 150 mm, 5 μm particles). Mobile phase consisted of a mixture of 18 MΩ deionized water (solvent A) and acetonitrile (solvent B, HPLC PLUS-Gradient from Carlo Erba, France) both containing 0.1% TFA. Elution was performed at 1 mL/min using a linear gradient from 40 to 62.5% solvent B over 15 min followed by column equilibration for 2 min after return to 40% solvent B in 3 min. Solutions of crude reaction mixtures and of purified compounds were systematically filtered beforehand through a membrane (0.45 μm, Macherey-Nagel) before being injected (20 μL injection volume). The chromatograms were recorded at 265 nm (λ_{max} of TCO- and $CCOPEG_{4/8/12,\ 3/7/11}$ carboxylic acids and NHS esters) and 286 nm (λ_{max} of TCO- and CCO−NHS). The TCO/CCO ratio was determined using the peak area ratio of TCO and CCO derivatives, compounds that were identified on the basis of their retention times when they were previously injected separately.

5.3. MALDI-ToF

Determination of the mean number of TCO moieties per mAb. Assessments were made using MALDI-TOF MS analyzes (Voyager DE-Pro mass spectrometer, Sciex, USA). Sinapinic acid (Sigma, France) was diluted in acetonitrile/water (30/70, v/v) with 0.1% TFA at 10 mg/mL to obtain the matrix solution. A set of three serial dilutions from 1 mg/mL of all mAb-PEG_x-TCO conjugates in PBS was prepared by mixing those latter with the matrix solution (2/1, v/v). Acquisitions were performed in a positive linear mode and 600 shots were averaged for each spectrum. The average molecular weight of mAb conjugates was obtained from the mass of the $[M+H]^+$ peak for the dilution set. Calibration settings corresponded to a close external mode using IgG1 (AB Sciex, USA). The number of TCO derivatives grafted per mAb was calculated using the molecular weight difference between the mAb-PEG_x-TCO conjugates and the unmodified mAbs, net masses added depending on the modification (about 272, 520 and 872 Da for **3**, **9a** and **9c** respectively). Final concentrations of mAb-PEG_x-TCO conjugates were measured using a Multiskan GO UV/Vis microplate spectrophotometer at $\lambda = 280$ nm (Thermo Fisher Scientific, France).

5.4. Immunofluorescence assays for trans-cis cyclooctene isomerization assay

8-well labtek chambers (Sigma Aldrich, France) were first coated at 5 μg/cm2 with rat tail collagen I (Corning, USA) during 1 h at RT. After washing 3 times with 400 μL of D-PBS to remove acetic acid, 1.10^5 A431-CEA-Luc cells, transfected for the expression of carcino-embryonic antigen (CEA) and Luciferase were incubated 48 h in chambers. Cells were cultured in Dulbecco's Modified Eagle F12 Medium supplemented with 10% fetal serum, 1% penicillin/streptomycin, 1% geneticin, 1% hygromycin at 37 °C with 5% CO_2 in humidified environment. For immunofluorescence experiments, cells were first incubated 30 min with D-PBS-BSA 5% at RT then 1.5 h at 37 °C/5% CO_2 with 0.03 nmol of the appropriate mixture of mAb (Ts29.2 without TCO; **Ts29.2@1a**; **Ts29.2@2a**; **Ts29.2@3a**; **Ts29.2@1b**; **Ts29.2@2b**; **Ts29.2@3b**; **Ts29.2@1c**; **Ts29.2@2c**; **Ts29.2@3c**) diluted in D-PBS-BSA 2.5%. After washing the cells twice with D-PBS to remove unfixed mAbs, they were incubated 45 min at 37 °C/5% CO_2 with either 1/1000 donkey anti-mouse antibody labeled with Cyanine 3 (Jackson ImmunoResearch, USA) diluted in D-PBS-BSA 2.5% or 10−14 equivalent of 3-(p-benzylamino)-1,2,4,5-tetrazine-cyanine3 (Tz-Cy3, absorbance/emission at 550/570 nm, Jena Bioscience, Germany) with respect to the number of TCO or CCO, diluted in D-PBS-BSA 2.5% - DMSO 0.5%. Cells were then washed 3 times with D-PBS and fixed with 10% formalin (Sigma Aldrich, France). Chambers were finally removed from the labteks and blades were mounted in vectashield-DAPI mounting medium. Signal observation was made using a confocal imager (Leica SPE, ICCF platform, Clermont-Ferrand, France). Region of interest (ROI) of three fields per well, all Z-sections every 2 μm, were randomly imaged and quantified on the entire image with ImageJ software using an automated 3D-strategy. For more details about the quantification method, please refer to our previous works [7,33].

5.5. In vitro mAb-TCO/CCO immunoconjugates reactivity

About 5 μg of Ts29.2 without TCO; **Ts29.2(PEG0)@1a**; **Ts29.2(PEG0)@2a**; **Ts29.2(PEG0)@3a**; **Ts29.2(PEG4)@1b**; **Ts29.2(PEG4)@2b**; **Ts29.2(PEG4)@3b**; **Ts29.2(PEG12)@1c**; **Ts29.2(PEG12)@2c**; **Ts29.2(PEG12)@3c** were added to D-PBS or plasma 50% diluted in D-PBS and then incubated during 1 h, 5 h or 24 h at 37 °C in a water bath with moderate agitation. After 1 h, 5 h or 24 h of incubation, each mixture of mAb was added to Laemli 4X and D-PBS, so as to reach a final volume of 20 μL. Afterwards, samples were directly loaded without any reducing agent on 4−15% SDS-PAGE acrylamide gels (Biorad, France) and after migration, gels were incubated 5 min under gentle shaking with 0.002 mM of 3-(p-benzylamino)-1.2.4.5-tetrazine-5-Fluorescein diluted in water (Tz-5-FAM, absorbance/emission wavelengths 492/517 nm, 10−14 equivalents with respect to TCO/CCO). After 10 min wash in water, gels were imaged with Chemidoc imager (Biorad, France) and then colored with Simplyblue™ SafeStain following the manufacturer's instructions (Thermofisher Scientific, France). Major band was quantified using ImageLab software, fluorescence intensity signal being normalized by the total amount of protein loaded.

Funding sources

J-B. B received a PhD fellowship of Clermont-Auvergne University. A.R. received a PhD fellowship from FEDER and Région Auvergne-Rhône-Alpes.

Declaration of competing interest

The authors declare that they have no known competing financial interests or personal relationships that could have appeared to influence the work reported in this paper.

Acknowledgment

We warmly thank Pr Mohamed Saraka (ICCF of Clermont-Fd, France) for the photochemical syntheses. Confocal imaging was performed at the CLIC platform of Clermont-Ferrand (France).

Appendix A. Supplementary data

Supplementary data to this article can be found online at https://doi.org/10.1016/j.ejmech.2020.112574.

Abbreviations

IEDDA	Inverse electronic demand Diels-Alder
RIT	radioimmunotherapy
TCO	trans-cyclooctene
CCO	cos-cyclooctene
PRIT	pretargeted radioimmunotherapy
SPECT	single photon emission computed tomography
PET	positron emission tomography
PEG	polyethylene glycol

TSPN8 tetraspanin8
SDS-PAGE sodium dodecyl sulfate polyacrylamide gel electrophoresis

References

[1] J.-P. Pouget, C. Lozza, E. Deshayes, V. Boudousq, I. Navarro-Teulon, Introduction to radiobiology of targeted radionuclide therapy, Front. Med. 2 (12) (2015) 1–12.
[2] J.-P. Pouget, I. Navarro-Teulon, M. Bardiès, N. Chouin, G. Cartron, A. Pèlegrin, D. Azria, Clinical radioimmunotherapy-the role of radiobiology, Nat. Rev. Clin. Oncol. 8 (12) (2011) 720–734.
[3] D.M. Goldenberg, C.-H. Chang, E.A. Rossi, W.J. McBride, R.M. Sharkey, Pretargeted molecular imaging and radioimmunotherapy, Theranostics 2 (5) (2012) 523–540.
[4] M. Patra, K. Zarschler, H.-J. Pietzsch, H. Stephan, G. Gasser, New insights into the pretargeting approach to image and treat tumours, Chem. Soc. Rev. 45 (23) (2016) 6415–6431.
[5] E.J.L. Stéen, P.E. Edem, K. Nørregaard, J.T. Jørgensen, V. Shalgunov, A. Kjaer, M.M. Herth, Pretargeting in nuclear imaging and radionuclide therapy: improving efficacy of theranostics and nanomedicines, Biomaterials 179 (2018) 209–245.
[6] C. Bailly, C. Bodet-Milin, C. Rousseau, A. Faivre-Chauvet, F. Kraeber-Bodéré, J. Barbet, Pretargeting for imaging and therapy in oncological nuclear medicine, EJNMMI Radiopharm. Chem. 2 (2017) 6.
[7] A. Rondon, F. Degoul, Antibody pretargeting based on bioorthogonal click chemistry for cancer imaging and targeted radionuclide therapy, Bioconjugate Chem. (2020), https://doi.org/10.1021/acs.bioconjchem.9b00761.
[8] P. Magnani, F. Fazio, C. Grana, C. Songini, L. Frigerio, S. Pecorelli, G. Mangili, N. Colombo, C.D.A. Mariani, G. Paganelli, Diagnosis of persistent ovarian carcinoma with three-step immunoscintigraphy, Br. J. Canc. 82 (3) (2000) 616–620.
[9] F. Kraeber-Bodéré, J. Barbet, J.-F. Chatal, Radioimmunotherapy: from current clinical success to future industrial breakthrough? J. Nucl. Med. 57 (3) (2016) 329–331.
[10] D.R. Stickney, L.D. Anderson, J.B. Slater, C.N. Ahlem, G.A. Kirk, S.A. Schweighardt, J.M. Frincke, Bifunctional antibody: a binary radiopharmaceutical delivery system for imaging colorectal carcinoma, Cancer Res 51 (24) (1991) 6650–6655.
[11] H.P. Kalofonos, M. Rusckowski, D.A. Siebecker, G.B. Sivolapenko, D. Snook, J.P. Lavender, A.A. Epenetos, D.J. Hnatowich, Imaging of tumor in patients with indium-111-labeled biotin and streptavidin-conjugated antibodies: preliminary communication, J. Nucl. Med. 31 (11) (1990) 1791–1796.
[12] P.L. Weiden, H.B. Breitz, O. Press, J.W. Appelbaum, J.K. Bryan, S. Gaffigan, D. Stone, D. Axworthy, D. Fisher, J. Reno, Pretargeted radioimmunotherapy (PRIT) for treatment of non-Hodgkin's lymphoma (NHL): initial phase I/II study results, Biother. Radiopharm. 15 (1) (2000) 15–29.
[13] G. Liu, S. Dou, Y. Liu, Y. Wang, M. Rusckowski, D.J. Hnatowich, ^{90}Y labeled phosphorodiamidate morpholino oligomer for pretargeting radiotherapy, Bioconjugate Chem. 22 (12) (2011) 2539–2545.
[14] K.D. Bagshawe, Antibody-directed enzyme prodrug therapy (ADEPT) for cancer, Expert Rev. Anticancer Ther. 6 (2006) 1421–1431.
[15] E.M. Sletten, C.R. Bertozzi, From mechanism to mouse: a tale of two bioorthogonal reactions, Acc. Chem. Res. 44 (9) (2011) 666–676.
[16] F.C.J. van de Watering, M. Rijpkema, M.S. Robillard, W.J.G. Oyen, O.C. Boerman, Pretargeted imaging and radioimmunotherapy of cancer using antibodies and bioorthogonal chemistry, Front. Med. 1 (44) (2014) 1–11.
[17] M.L. Blackman, M. Royzen, J.M. Fox, Tetrazine ligation: fast bioconjugation based on inverse-electron-demand Diels–Alder reactivity, J. Am. Chem. Soc. 130 (41) (2008) 13518–13519.
[18] J. Dommerholt, F.P.J.T. Rutjes, F.L. van Delft, Strain-promoted 1,3-dipolar cycloaddition of cycloalkynes and organic azides, Top. Curr. Chem. 374 (2) (2016) 16.
[19] R. Rossin, P.R. Verkerk, S.M. van den Bosch, R.C. Vulders, I. Verel, J. Lub, M.S. Robillard, In vivo chemistry for pretargeted tumor imaging in live mice, Angew Chem. Int. Ed. Engl. 49 (19) (2010) 3375–3378.
[20] B.M. Zeglis, P. Mohindra, G.I. Weissmann, V. Divilov, S.A. Hilderbrand, R. Weissleder, J.S. Lewis, Modular strategy for the construction of radiometalated antibodies for positron emission tomography based on inverse electron demand diels–alder click chemistry, Bioconjugate Chem. 22 (10) (2011) 2048–2059.
[21] R. Rossin, M.S. Robillard, Pretargeted imaging using bioorthogonal chemistry in mice, Curr. Opin. Chem. Biol. 21 (2014) 161–169.
[22] R.M. Rahim, R. Kota, J.B. Haun, Enhancing reactivity for bioorthogonal pretargeting by unmasking antibody-conjugated trans-cyclooctenes, Bioconjugate Chem. 26 (2) (2015) 352–360.
[23] J.P. Meyer, J.L. Houghton, P. Kozlowski, D. Abdel-Atti, T. Reiner, N.V. Pillarsetty, W.W. Scholz, B.M. Zeglis, J.S. Lewis, ^{18}F-Based pretargeted PET imaging based on bioorthogonal diels–alder click chemistry, Bioconjugate Chem. 27 (2) (2016) 298–301.
[24] J.L. Houghton, R. Membreno, D. Abdel-Atti, K.M. Cunanan, S. Carlin, W.W. Scholz, P.B. Zanzonico, J.S. Lewis, B.M. Zeglis, Establishment of the in vivo efficacy of pretargeted radioimmunotherapy utilizing inverse electron demand diels-alder click chemistry, Mol. Canc. Therapeut. 16 (1) (2017) 124–133.
[25] R. Rossin, T. Läppchen, S.M. van den Bosch, R. Laforest, M.S. Robillard, Diels–alder reaction for tumor pretargeting: in vivo chemistry can boost tumor radiation dose compared with directly labeled antibody, J. Nucl. Med. 54 (11) (2013) 1989–1995.
[26] T. Läppchen, R. Rossin, T.R. van Mourik, G. Gruntz, F.J.M. Hoeben, R.M. Versteegen, H.M. Janssen, J. Lub, M.S. Robillard, DOTA-tetrazine probes with modified linkers for tumor pretargeting, Nucl. Med. Biol. 55 (2017) 19–26.
[27] S. Kronister, D. Svatunek, C. Denk, H. Mikula, Acylation-mediated 'kinetic turn-on' of 3-Amino-1,2,4,5-tetrazines, Synlett 29 (10) (2018) 1297–1302.
[28] A.P. Chapman, PEGylated antibodies and antibody fragments for improved therapy: a review, Adv. Drug Deliv. Rev. 54 (4) (2002) 531–545.
[29] E. Kozma, I. Nikić, B.R. Varga, I.V. Aramburu, J.H. Kang, O.T. Fackler, E.A. Lemke, Hydrophilic trans-cyclooctenylated noncanonical amino acids for fast intracellular protein labeling, Chembiochem 17 (2016) 1518–1524.
[30] R. Rossin, S.M. van den Bosch, W. Ten Hoeve, M. Carvelli, R.M. Versteegen, J. Lub, M.S. Robillard, Highly reactive trans-cyclooctene tags with improved stability for diels–alder chemistry in living systems, Bioconjugate Chem. 24 (7) (2013) 1210–1217.
[31] S. Poty, R. Membreno, J.M. Glaser, A. Ragupathi, W.W. Scholz, B.M. Zeglis, J.S. Lewis, The inverse electron-demand Diels–Alder reaction as a new methodology for the synthesis of ^{225}Ac-labelled radioimmunoconjugates, Chem. Commun. 54 (21) (2018) 2599–2602.
[32] R. Rossin, S.M. van Duijnhoven, T. Läppchen, S.M. van den Bosch, M.S. Robillard, Trans-cyclooctene tag with improved properties for tumor pretargeting with the diels–alder reaction, Mol. Pharm. 11 (9) (2014) 3090–3096.
[33] A. Rondon, N. Ty, J.-B. Bequignat, M. Quintana, A. Briat, T. Witkowski, B. Bouchon, C. Boucheix, E. Miot-Noirault, J.P. Pouget, J.M. Chezal, I. Navarro-Teulon, E. Moreau, F. Degoul, Antibody PEGylation in bioorthogonal pretargeting with trans-cyclooctene/tetrazine cycloaddition: in vitro and in vivo evaluation in colorectal cancer models, Sci. Rep. 7 (1) (2017), 14918.
[34] A. Rondon, S. Schmitt, A. Briat, N. Ty, L. Maigne, M. Quintana, R. Membreno, B.M. Zeglis, I. Navarro-Teulon, J.P. Pouget, J.M. Chezal, E. Miot-Noirault, E. Moreau, F. Degoul, Pretargeted radioimmunotherapy and SPECT imaging of peritoneal carcinomatosis using bioorthogonal click chemistry: probe selection and first proof-of-concept, Theranostics 9 (22) (2019) 6706–6718.
[35] B.E. Cook, R. Membreno, B.M. Zeglis, Dendrimer scaffold for the amplification of in vivo pretargeting ligations, Bioconjugate Chem. 29 (8) (2018) 2734–2740.
[36] M. Royzen, G.P.A. Yap, J.M. Fox, A photochemical synthesis of functionalized trans-cyclooctenes driven by metal complexation, J. Am. Chem. Soc. 130 (12) (2008) 3760–3761.
[37] E.M.F. Billaud, E. Shahbazali, M. Ahamed, F. Cleeren, T. Noël, M. Koole, A. Verbruggen, V. Hessel, G. Bormans, Micro-flow photosynthesis of new dienophiles for inverse-electron-demand Diels–Alder reactions. Potential applications for pretargeted in vivo PET imaging, Chem. Sci. 8 (2) (2017) 1251–1258.
[38] B.M. Zeglis, K.K. Sevak, T. Reiner, P. Mohindra, S.D. Carlin, P. Zanzonico, R. Weissleder, J.S.A. Lewis, Pretargeted PET imaging strategy based on bioorthogonal diels-alder click chemistry, J. Nucl. Med. 54 (8) (2013) 1389–1396.
[39] A. Yazdani, H. Bilton, A. Vito, A.R. Genady, S.M. Rathmann, Z. Ahmad, N. Janzen, S. Czorny, B.M. Zeglis, L.C. Francesconi, J.F. Valliant, A bone-seeking trans-cyclooctene for pretargeting and bioorthogonal chemistry: a proof of concept study using 99mTc- and 177Lu-labeled tetrazines, J. Med. Chem. 59 (20) (2016) 9381–9389.
[40] K. Fujiki, Y. Kanayama, S. Yano, N. Sato, T. Yokokita, P. Ahmadi, Y. Watanabe, H. Haba, K. Tanaka, ^{211}At-labeled immunoconjugate via a one-pot three-component double click strategy: practical access to α-emission cancer radiotherapeutics, Chem. Sci. 10 (7) (2018) 1936–1944.
[41] A. Darko, S. Wallace, O. Dmitrenko, M.M. Machovina, R.A. Mehl, J.W. Chin, J.M. Fox, Conformationally strained trans-cyclooctene with improved stability and excellent reactivity in tetrazine ligation, Chem. Sci. 5 (10) (2014) 3770–3776.
[42] E.J.L. Stéen, J.T. Jørgensen, K. Johann, K. Nørregaard, B. Sohr, D. Svatunek, A. Birke, V. Shalgunov, P.E. Edem, R. Rossin, C. Seidl, F. Schmid, M.S. Robillard, J.L. Kristensen, H. Mikula, M. Barz, A. Kjær, M.M. Herth, Trans-cyclooctene-functionalized PeptoBrushes with improved reaction kinetics of the tetrazine ligation for pretargeted nuclear imaging, ACS Nano (2020), https://doi.org/10.1021/acsnano.9b06905.
[43] S.M. Cheal, M. Patel, G. Yang, D.R. Veach, H. Xu, H.F. Guo, P.B. Zanzonico, D.B. Axworthy, N.K. Cheung, O. Ouerfelli, S.M. Larson, A N-acetylgalactosamino dendron-clearing agent for high-therapeutic index DOTA-hapten pretargeted radioimmunotherapy, Bioconjugate Chem. (2019), https://doi.org/10.1021/acs.bioconjchem.9b00736.
[44] R. Membreno, B.E. Cook, K. Fung, J.S. Lewis, B.M. Zeglis, Click-mediated pretargeted radioimmunotherapy of colorectal carcinoma, Mol. Pharm. 15 (4) (2018) 1729–1734.
[45] R. Membreno, O.M. Keinänen, B.E. Cook, K.M. Tully, K.C. Fung, J.S. Lewis, B.M. Zeglis, Toward the optimization of click-mediated pretargeted radioimmunotherapy, Mol. Pharm. 16 (5) (2019) 2259–2263.